

LASER SPECTROSCOPY

PACS numbers: 42.62.Eh; 42.62.Fi; 37.10.De; 37.10.Gh
DOI: 10.1070/QE2015v045n02ABEH015638

Spectroscopy of intercombination transition $^1S_0-{}^3P_1$ for secondary cooling of strontium atoms

K.Yu. Khabarova, A.A. Galyshev, S.A. Strelkin, A.S. Kostin,
G.S. Belotelov, O.I. Berdasov, A.Yu. Gribov, N.N. Kolachevsky, S.N. Slyusarev

Abstract. **In the framework of the project aimed at creating an optical standard on cold Sr atoms we have realised sub-Doppler spectroscopy of the intercombination transition $^1S_0-{}^3P_1$ (689 nm) in a cell with Sr vapour and in a cloud of atoms loaded in a magneto-optical trap (MOT). By measuring Zeeman splitting of the $^3P_1$ level in the magnetic field of the MOT we have succeeded in fine adjustment of the MOT relative to a minimum of the magnetic field, which is necessary for successful secondary-stage cooling on the intercombination transition. In turn, absorption saturation spectroscopy in the vapour cell provides the long-term frequency stability of the second-stage cooling laser at λ = 689 nm.**

Keywords: *optical clock, strontium, saturation absorption spectroscopy, magneto-optical trap.*

1. Introduction

Progress in the methods of atom trapping and confinement, stabilising laser operation and in measurements of optical frequencies has resulted in impetuous enhancement of atomic clock performance both in the microwave and optical ranges. Investigations in the field of atomic clock gave a stimulus to development of advanced fields of science and affected progress in fundamental and applied investigations. In recent years, optical frequency standards on neutral atoms trapped in optical lattice have become superior to standards on single ions by accuracy and stability. In 2013, A. Ludlow et al. [1] demonstrated the record relative stability in comparing two ytterbium clocks (the Allan variance was $\sigma_y = 1.6\times10^{-18}$ at the averaging time of 7 hours [1]), and a group headed by J. Ye reported the record relative stability in comparing two strontium clocks ($\sigma_y = 1.6\times10^{-18}$ at the averaging time of 10000 s [2]). A clock on strontium atoms exhibits the highest self-consistency [3, 4], which led the Comité International des Poids et Mesures to recommend such a clock for SI second redifinition. In Russia, works on development of optical clocks on strontium-87 isotope loaded to an optical trap are carried out in VNIIFTRI in the frameworks of Federal Central Programme 'GLONASS' [5].

By forming an optical lattice at the 'magic' wavelength one can cancel the linear part of the dynamic Stark frequency shift for clock transition [6, 7], and the choice of polarisation can minimise high-order corrections [8]. For Sr and Yb atoms, the 'magic' wavelengths are in the range covered by the laser sources, which are available and can form sufficiently deep optical lattices.

In order to provide atom confinement (in the Lamb–Dicke regime) the optical lattice should be sufficiently deep. However, an increased depth results in a greater residual contribution from the dynamic Stark effect, and therefore the working depth of lattice is usually chosen less than $100E_{\rm rec}$, where $E_{\rm rec}$ = 0.1 μK is the recoil energy for the lattice wavelength $\lambda_{\rm L}$. Hence, in order to efficiently load atoms to an optical lattice it is necessary to deeply cool atoms to temperatures below 10 μK. The structure of energy levels of the strontium atom is suitable for laser cooling in two stages. The primary cooling is performed by the classical method of laser cooling on the spectrally broad allowed transition $^1S_0-{}^1P_1$ which has the natural linewidth γ_1 = 30 MHz and wavelength of 461 nm. In this case, temperatures of 1–3 mK (the Doppler limit is $T_{\rm D} = h\gamma_1/2k_{\rm B}$ = 770 μK) can be reached, which corresponds to the thermal velocities of approximately 1 m s^{-1} [9]. The method has no specific requirements, and our team has successfully employed it in 2011 [10]. However, such temperatures are too high for efficient loading of atoms to the optical lattice, and further cooling is needed. The electron shell in the ground state of strontium atom has no magnetic moment, which makes methods of sub-Doppler cooling widely used for alkali atoms [11] inefficient.

Deep (secondary) cooling of strontium atoms uses the intercombination transition $^1S_0-{}^3P_1$ at the wavelength of 689 nm with the natural linewidth γ_2 = 7.4 kHz. The Doppler limit for this transition is 200 nK, but laser cooling on such narrow transition imposes strong constraints on the spectrum

K.Yu. Khabarova Federal State Unitary Enterprise 'All-Russian Scientific-Research Institute of Physical-Technical and Radiotechnical Measurements', 141570 Mendeleevo, Moscow region, Russia; P.N. Lebedev Physics Institute, Russian Academy of Sciences, Leninsky prosp. 53, 119991 Moscow, Russia; e-mail: kseniyakhabarova@gmail.com;
A.A. Galyshev, S.A. Strelkin, O.I. Berdasov, A.Yu. Gribov Federal State Unitary Enterprise 'All-Russian Scientific-Research Institute of Physical-Technical and Radiotechnical Measurements', 141570 Mendeleevo, Moscow region, Russia; National Research Nuclear University 'MEPhI', Kashirskoye shosse 31, 123182 Moscow, Russia; e-mail: galyshev89@gmail.com, sergo6989@gmail.com, berd_7@mail.ru, gribov.art@mail.ru;
A.S. Kostin, G.S. Belotelov, S.N. Slyusarev Federal State Unitary Enterprise 'All-Russian Scientific-Research Institute of Physical-Technical and Radiotechnical Measurements', 141570 Mendeleevo, Moscow region, Russia; e-mail: askostin.mipt@yandex.ru, serslyu@mail.ru;
N.N. Kolachevsky Federal State Unitary Enterprise 'All-Russian Scientific-Research Institute of Physical-Technical and Radiotechnical Measurements', 141570 Mendeleevo, Moscow region, Russia; P.N. Lebedev Physics Institute, Russian Academy of Sciences, Leninsky prosp. 53, 119991 Moscow, Russia; National Research Nuclear University 'MEPhI', Kashirskoye shosse 31, 123182 Moscow, Russia; e-mail: kolachbox@mail.ru

Received 21 July 2014; revision received 29 September 2014
Kvantovaya Elektronika **45** (2) 166–170 (2015)
Translated by N.A. Raspopov

of laser radiation, its frequency stability, and requires compensation and high symmetry of magnetic fields in the magneto-optical trap (MOT). This is why investigation of this transition is important in realising reliable secondary cooling.

The transition has been studied in a number of works by other research groups [12–14]. In the present work, in addition to a number of original technical solutions concerning spectroscopy of strontium atoms in a cell, we suggest a new method for adjusting the MOT by observing Zeeman splitting of the level $^3P_1$ in a cloud of preliminarily cooled strontium atoms at a wavelength of 461 nm.

2. Experimental setup and primary cooling of strontium-88 atoms

We have realised the scheme of the primary MOT (461 nm) in three pairs of anti-collinear orthogonal beams, which intersect at a centre of the titanium vacuum chamber, schematically shown in Fig. 1a. Strontium atoms emitted by the thermal source are preliminarily slowed down in Zeeman slower to velocities of about 20 m s^{-1}. The beams of the primary MOT intersect at the trap centre (in Fig. 1, the third pair of beams is directed normal to the plane of figure and is denoted by a black circle) and form a cloud from the flow of slowed atoms. Relative intensities of the laser beams at the cooling wavelength $\lambda = 461$ nm are 3:3:1 ($x:y:z$), which provides formation of the most symmetric cloud. The magnetic field inside the MOT is formed by two coils of anti-Helmholtz configuration with the axis directed along the z axis. The coils are made of a hollow copper pipe of diameter 4 mm with kapton insulation. Cooling water is supplied through a tube under high pressure, which allows one to increase the coil current to 70 A and to reach the magnetic field gradient at the chamber centre of up to 120 Gs cm^{-1}. The value of the gradient that is sufficient for capturing a maximal number of atoms in the MOT is 50 Gs cm^{-1}.

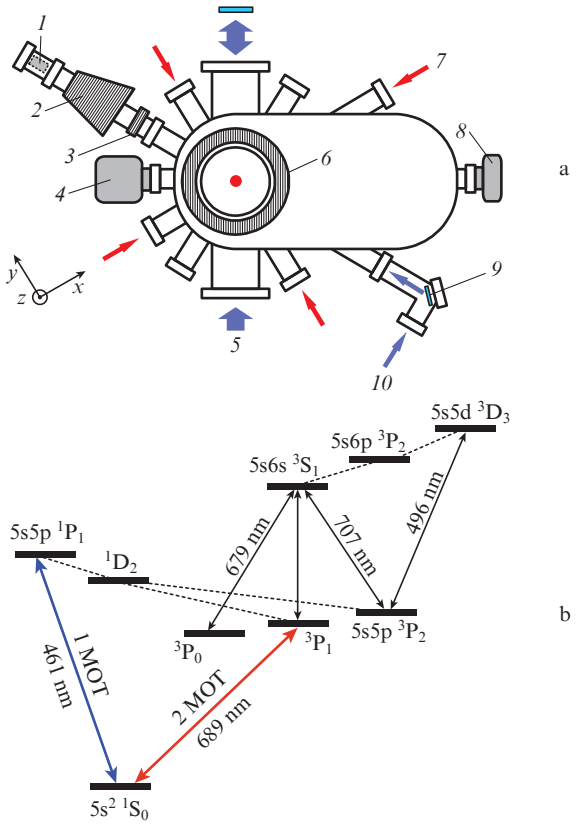

Figure 1. (a) Schematic diagram of the vacuum chamber [(*1*) evaporation oven; (*2*) Zeeman slower; (*3*) bucking coil; (*4*) PEM; (*5*) illuminating beam; (*6*) MOT coils; (*7*) MOT beams (461 and 689 nm); (*8*) CCD-camera; (*9*) silver mirror; (*10*) Zeeman beam (461 nm)] and (b) the levels of the strontium atom involved in the processes of laser cooling.

A large gradient of the magnetic field in the primary MOT prevents laser cooling on the intercombination transition, and therefore in the process of secondary cooling the field gradient should be rapidly lowered down to 3 Gs cm^{-1}. Since the characteristic time-off for atoms in the primary trap is several milliseconds, it is necessary to quickly switch off the field while passing to the stage of secondary cooling. For this purpose the coils are equipped with the electronic system on field-effect transistors capable of switching off the magnetic field in a characteristic time of 0.5 ms.

Laser radiation for Zeeman slower and MOT beams is provided by a TA-SHG pro semiconductor system (Toptica), which includes a diode laser with an external cavity, a semiconductor amplifier and a second-harmonic converter unit. The system provides the radiation power of up to 450 mW at $\lambda = 461$ nm with the spectral width of 2 MHz. The laser frequency is stabilised by a high-stability commercial WS-U interferometer (Angstrom), which is calibrated by an Orvilas-532-5-C laser standard with iodine cell. Ballistic measurements and detection in the secondary trap are performed with illuminating light resonant to the $^1S_0-^1P_1$ transition. The beams have equal intensities and are anti-collinear in order to minimise their influence on the cloud.

For fast switching on and off the illuminating radiation, primary MOT and Zeeman slower, laser radiation passes through acousto-optical modulators (AOMs) which operate in the first diffraction order and shift the radiation frequency by 40, 120 and 770 MHz, respectively. The radio-frequency signals feeding AOMs pass through the switches controlled by digital pulses so that radiation can be switched on or off in a time interval of less than 1 μs. Since the AOM in a single-pass scheme can suppress power by only 30–40 dB, mechanical shutters with a switching time of 0.5 ms are additionally used to provide complete light blocking. Experiment is controlled (forming control signals for AOMs, shutters, magnetic field, and data acquisition) by means of the LabView software package, which provides signal synchronisation at the level of 1 μs.

Detection of luminescence from atoms at the wavelength of 461 nm is made by a PEM onto which a part of the trap volume is reflected. The image of the cloud is also recorded by a CCD-camera controlled by a computer.

With the system described above, the primary laser cooling has been observed for all strontium atom isotopes: ^{84}Sr (0.56%), ^{86}Sr (9.86%), ^{87}Sr (7.02%) and ^{88}Sr (82.56%) [10]. Below we will investigate the secondary cooling transition of mostly abundant isotope ^{88}Sr, on which the methods of cooling and spectroscopy are refined.

3. Absorption saturation spectroscopy of the transition of secondary cooling in a cell

For tuning to the weak intercombination transition $^1S_0-^3P_1$ and compensating drift of laser frequency at long times we have realised the scheme of saturated absorption spectros-

copy of the $^1S_0-^3P_1$ transition in vapours of strontium atoms in a cell. Since the transition natural width is small (γ_2 = 7.4 kHz) the sub-Doppler spectroscopy requires narrowing the spectrum of the 689-nm exciting TA-pro laser (Toptica) with the initial width of 1 MHz. This was made by using a high-Q ULE-cavity capable of obtaining the spectral width of laser radiation as narrow as 100 Hz at the frequency drift of less than 1 Hz s^{-1} [15].

A scheme of the experimental setup for studying saturated absorption spectroscopy of intercombination transition in a cell is presented in Fig. 2. Before entering the cell, the laser radiation beam is split into the saturation and probe beams which are introduced into the cell exactly in opposite directions in parallel linear polarisations. The saturation beam is modulated in amplitude by the AOM, whereas the signal in the probe beam is recorded by a synchronous detector at the modulation frequency.

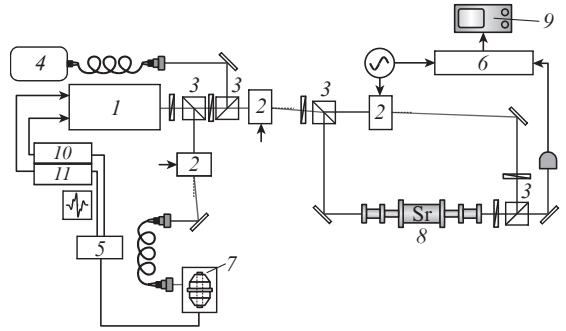

Figure 2. Scheme of the experiment on saturation absorption spectroscopy of the $^1S_0-^3P_1$ transition in vapours of Sr atoms in a cell: (*1*) 689-nm laser; (*2*) AOM; (*3*) polarisation cube; (*4*) WS-U wavemeter; (*5*) unit forming the feedback error signal; (*6*) synchronous detector; (*7*) ULE-cavity; (*8*) cell; (*9*) oscilloscope; (*10*) piezoceramics; (*11*) current.

The cell is a tube made of stainless steel of diameter 20 mm (adapter) and 35 mm (central part) with the total length of 55 cm (Fig. 3). Windows made of fused quartz with an antireflection coating to the wavelength of 689 nm are attached to the ends of the cell. Several strontium pieces of diameter about 5 mm are placed at the centre of cell. Sufficient optical density requires intensive heating, in which case strontium vapours may deposit optical windows and become a serious technical problem. At a temperature of about 500 °C (the characteristic working temperature in the experiment) the saturated vapour pressure is 1 Pa.

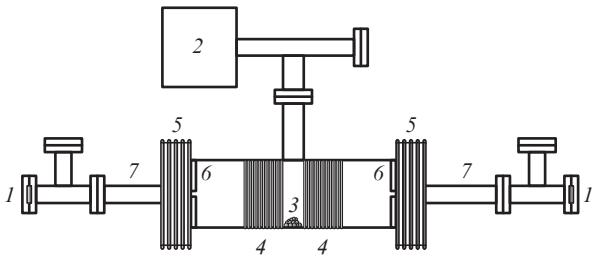

Figure 3. Cell for saturation absorption spectroscopy: (*1*) window; (*2*) ion-getter pump; (*3*) Sr; (*4*) thermo-cable; (*5*) water cooler; (*6*) iris; (*7*) adapter.

Twenty turns of a heating wire were wound on the central part of the cell. To prevent heating of the whole cell and to cool its ends with mounted irises and nearby cell parts, six turns of a copper pipe were wound on the cell periphery parts with water flowing through the pipe. A central part of the cell is continuously pumped by an ion-getter Varian pump with the efficiency of 2 L s^{-1} to a pressure of $\sim 10^{-6}$ mbar.

In the first cell design the pump was placed near one of windows. In that case the window transmission rapidly deteriorated due to strontium deposition. After placing the pump to the centre of cell the windows were no more deposited with strontium. This is explained by a sufficiently high buffer gas pressure near windows (differential pumping), which prevents strontium atoms from moving to windows.

In Fig. 4 one can see spectra of saturated absorption for the strontium transition $^1S_0-^3P_1$ at two powers of the saturation beam. The magnetic field at the cell centre formed by the heater makes it possible to select the magnetically insensitive transition between Zeeman components $^1S_0(m_j = 0) \rightarrow {}^3P_1$ ($m_j = 0$). The transition is broadened by power, because the intensity of incident radiation is substantially greater than the saturation intensity.

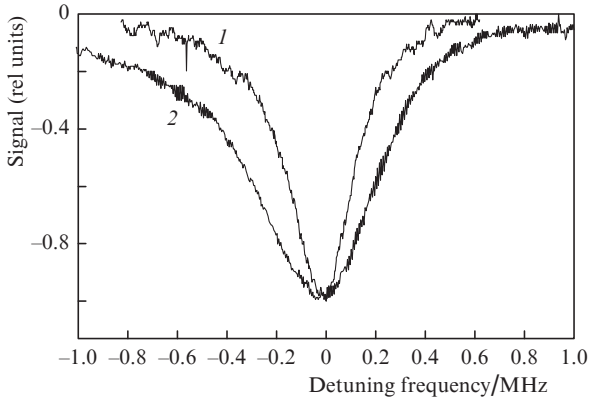

Figure 4. Spectra of saturated absorption of strontium-88 vapours on the $^1S_0$ ($m_j = 0$) → $^3P_1$ ($m_j = 0$) transition obtained at the power of (*1*) 13 mW and (*2*) 100 mW in the saturation beam.

The dependence of the full width at half maximum for the spectral line (fitted by the Lorentz profile) on the saturation beam power is presented in Fig. 5. Extrapolation to the zero power gives the resonance width of 280 kHz. This value corresponds to the time-of-flight broadening in the laser beams.

In order to enhance the laser frequency stability, a phase electro-optical modulator has been introduced to the scheme in Fig. 2, which provided recording of dispersion profiles (derivatives of spectra in Fig. 4). The laser frequency was stabilised with respect to the dispersion profile centre, which yielded the long-term frequency stability of about 50 kHz, sufficient for the process of secondary cooling.

Thus, the laser was adjusted to the transition of secondary cooling, and the long-term stability of its frequency (at time intervals longer than 1 hour) was provided by the cell. At shorter time intervals the laser frequency stability was determined by the ULE-cavity [15].

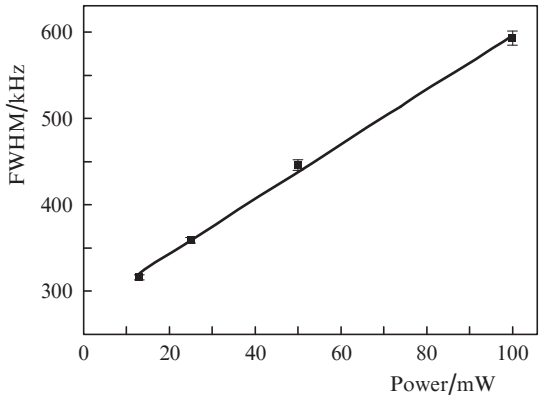

Figure 5. Resonance FWHM as a function of the saturation beam power.

4. Spectroscopy of the $^1S_0-^3P_1$ transition in laser-cooled atoms of strontium-88

Reloading of preliminarily cooled Sr atoms to the secondary trap and realisation of secondary cooling require that the cloud of pre-cooled Sr atoms was exactly at the magnetic field minimum (zero). Due to imperfect symmetry of the magnetic system, unbalanced intensities and polarisations of cooling beams, atoms are usually located beyond the desired domain. The conventional adjustment method by the expansion of the primary cloud (symmetric expansion corresponds to the most symmetric configuration) is not sufficiently sensitive due to a relatively large cloud size and high velocities of the atoms.

We have realised the scheme of atom spectroscopy in the primary trap by using laser radiation with the wavelength of 689 nm. The scheme of energy levels in Fig. 1b shows that switching on the resonance field in the $^1S_0-^3P_1$ transition results in a partial transfer of the population from level $^1S_0$ to $^3P_1$ and, correspondingly, in the reduction of luminescence of the primary MOT, which operates on the strong transition $^1S_0-^1P_1$ (461 nm). The sensitivity was increased by using the method of synchronous detection (Fig. 6) with amplitude modulation of laser radiation at the wavelength of 689 nm by the AOM at the frequency of 10 kHz. The modulated beam of power 0.1–2 mW passed to the primary trap. The signal of luminescence at the wavelength λ = 461 nm was detected by the PEM and directed to a synchronous detector.

The characteristic spectrum of luminescence on the $^1S_0-^3P_1$ transition in the primary strontium trap recorded by the method described above is shown in Fig. 7. The power of cooling radiation in this case was about $10I_{sat}$ (I_{sat} = 9.5 μW cm^{-2} is the saturation intensity of the transition). In the spectrum one can see three peaks, which correspond to Zeeman splitting of the upper level $^3P_1$ in the magnetic field of the MOT at the axial field gradient of 50 Gs cm^{-1}. The shift of magneto-sensitive transitions $m_j = 0 \rightarrow m_j = \pm 1$ in the magnetic field was 2.1 MHz Gs^{-1}, whereas the sensitivity of the transition $0 \rightarrow 0$ to the magnetic field was negligible. The Rabi splitting [16], which insignificantly contributes into the spectrum structure has not been taken into account in modelling.

Although under the ideal balance of light beam intensities the trap should be in a zero magnetic field, a finite size of the trap results in that atoms in peripheral parts undergo Zeeman splitting. We have performed modelling making allowance for a spatial distribution of atoms in a gradient field. A large number of parameters (exact position of the cloud, spatial distribution of atoms and polarisation of probe radiation at 698 nm) hindered accurate simulation of experimental data; however, calculation results qualitatively represent the experimental curve from Fig. 7.

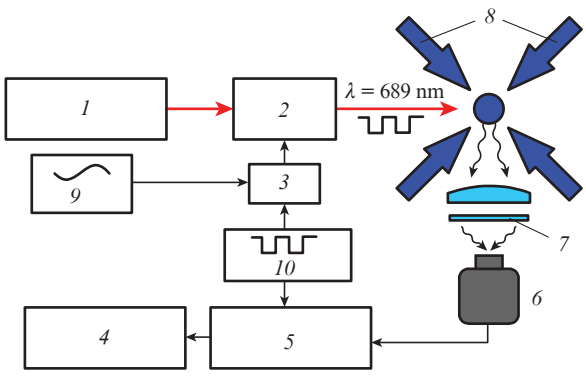

Figure 6. Scheme of the experiment on the spectroscopy of the $^1S_0-^3P_1$ transition in the primary strontium trap:
(*1*) 689-nm laser; (*2*) AOT; (*3*) switch; (*4*) oscilloscope; (*5*) synchronous detector; (*6*) PEM; (*7*) interference filter at λ = 461 nm; (*8*) MOT beams (461 nm); (*9*) AOT driver, frequency of 40 MHz; (*10*) rectangular pulse generator, frequency of 10 kHz.

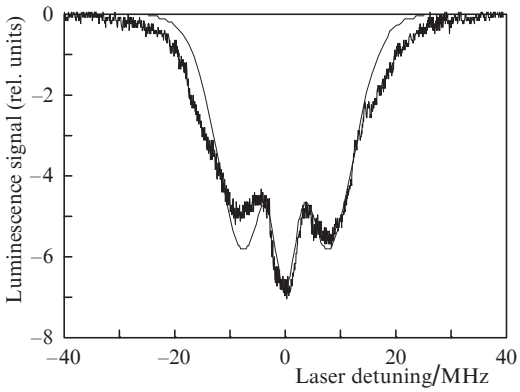

Figure 7. Luminescence intensity (461 nm) of a cloud of strontium-88 atoms in the MOT as a function of the detuning of the 689-nm laser from the $^1S_0-^3P_1$ transition resonance. Splitting of the magnetic components of the $^3P_1$ levels ($m_j = 0, \pm 1$) in the magnetic field of the MOT is observed. Thin curve is the fitting of the experimental data by the calculated curve described in the text.

According to the model, the shape of the central peak is close to the Gaussian profile with the width of 3 MHz at the level of $1/e^2$. The side peaks are substantially wider (10^{-11} MHz) due to the inhomogeneity of the magnetic field. Relative amplitudes of the side peaks are determined by the interaction with radiation of various polarisations at λ = 689 nm (with respect to the direction of local magnetic field), which depends on the position of the cloud relative to the minimum of the magnetic field. This parameter was used for adjusting the system.

The spectral width of the central peak (3–5 MHz, depending on experimental parameters) is mainly determined by the Doppler distribution in the primary trap. The temperature estimated from Doppler broadening is 5–10 mK, which cor-

responds to measurements performed by the ballistic method [10]. A noticeable excess of temperature over the Doppler limit is explained by high intensity of cooling beams. The characteristic splitting of magnetic components corresponds to the cloud radius of 0.8 mm at the axial field gradient of 50 Gs cm^{-1}, which confirms observations performed by the CCD-camera.

By observing the positions and symmetry of the side peaks (Fig. 7) we have performed accurate adjustment of trap position relative to the minimum of the magnetic field by compensating the magnetic fields and choosing intensities and polarisations of cooling radiation at λ = 461 nm. Thus, we have successfully realised secondary cooling of strontium-88 atoms.

5. Conclusions

Results of sub-Doppler spectroscopy of the $^1S_0-^3P_1$ transition in Sr atoms used for their secondary cooling down to a temperature of 1 μK are presented. In realising the cooling, the small natural width of this intercombination transition (7.4 kHz) introduces substantial experimental problems, which have been solved in the present work. The original reliable construction of the cell has been developed for the saturation absorption spectroscopy with oncoming beams, which was used for studying spectra of the $^1S_0-^3P_1$ transition and ensuring long-term stabilisation of the laser frequency system with the adjustment accuracy no worse than 50 kHz. Absorption spectra of the $^1S_0-^3P_1$ transition in the primary trap of Sr atoms have been measured, which allowed us, using Zeeman splitting of the $^3P_1$ level, to accurately adjust the primary trap by positioning it symmetrically relative to the zero magnetic field. The investigation carried out has made it possible to successively realise the secondary cooling of strontium-88 atoms at the wavelength of 689 nm, which will be described in following publications.

Acknowledgements. The work was partially supported by the Russian Foundation for Basic Research (Grant No. 12-02-01374).

References

1. Hinkley N., Sherman J.A., Phillips N.B., Schioppo M., Lemke N.D., Beloy K., Pizzocaro M., Oates C.W., Ludlow A.D. *Science*, **341** (6151), 1215 (2013).
2. Bloom B.J., Nicholson T.L., Williams J.R., Campbell S.L., Bishof M., Zhang X., Zhang W., Bromley S.L., Ye J. *Nature*, **506**, 71 (2014).
3. Blatt S. et. al. *Phys. Rev. Lett.*, **100**, 140801 (2008).
4. Campbell G.K. et.al. *Metrologia*, **45**, 539 (2008).
5. Slyusarev S.N., Kostin A.S., Baryshev V.N., Khabarova K.L., Pal'chikov V.G., Strelkin S.N. *Mir izmerenii*, **4**, 26 (2012).
6. Takamoto M., Hong F.L., Higashi R., Katori H. *Nature*, **435**, 321 (2005).
7. Katori H., Takamoto M., Pal'chiko V.G., Ovsiannikov V.D. *Phys. Rev. Lett.*, **91**, 173005 (2003).
8. Takamoto M., Katori H., Marmo S.I., Ovsiannikov V.D., Pal'chikov V.G. *Phys. Rev. Lett.*, **102**, 063002 (2009).
9. Ludlow A.D. *Ph.D. Theses* (University of Colorado, Boulder, 2008); http://jila.colorado.edu/yelabs/pubs/theses/2008/theses_2008_AndrewLudlow.pdf.
10. Slyusarev S., Kostin A., Barychev S., Khabarova K., Strelkin S., Donchenko S., Palchikov V., Krasavin A. *Book of Abstracts* (ICAP, 2012) p. 223.
11. Castin Y., Dalibard J., Cohen-Tannoudji C. *Bose-Einstein Condensation* (Cambridge: Cambridge Univ. Press, 1995).
12. Katori H., Ido T., Isoya Y., Kuwata-Gonokami M. *Phys. Rev. Lett.*, **82**, 1116 (1999).
13. Poli N., Drullinger R.E., Ferrari G., Leonard J., Sorrentino F., Tino G.M. *Phys.Rev. A*, **71**, 061403 (2005).
14. Loftus T.H., Ido T., Ludlow A.D., Boyd M.M., Ye J. *Phys. Rev. Lett.*, **93**, 073003 (2004).
15. Khabarova K.Yu., Slyusarev S.N., Strelkin S.A., Belotelov G.S., Kostin A.S., Pal'chikov V.G., Kolachevskii N.N. *Kvantovaya Electron.*, **42**, 1021 (2012) [*Quantum Electron.*, **42**, 1021 (2012)].
16. Akimov A.V., Tereshchenko E.O., Snigirev S.A., Samokotin A.Yu., Sokolov A.V., Sorokin V.N. *Kvantovaya Electron.*, **40**, 139 (2010) [*Quantum Electron.*, **40**, 139 (2010)].